



Contribution to the Themed Section: 'Plugging spatial ecology into sustainable fisheries and EBM' Original Article

Ocean destratification and fish evacuation caused by a Mid-Atlantic tropical storm

David H. Secor^{1*}, Fan Zhang², Michael H. P. O'Brien¹, and Ming Li²

¹Chesapeake Biological Laboratory, University of Maryland Centre for Environmental Science, Solomons, MD, USA

²Horn Point Laboratory, University of Maryland Centre for Environmental Science, Cambridge, MD, USA

*Corresponding author: tel: 410-326-7229; e-mail: secor@cbl.umces.edu.

Secor, D. H., Zhang, F., O'Brien, M. H. P., and Li, M. Ocean destratification and fish evacuation caused by a Mid-Atlantic tropical storm. – ICES Journal of Marine Science, 76: 573–584.

Received 4 October 2017; revised 13 November 2017; accepted 27 November 2017; advance access publication 5 January 2018.

Tropical and extratropical storms commonly occur in the Northwest Atlantic Ocean, sometimes causing catastrophic losses to coastal fisheries. Still, their influence on fish movements and range shifts is poorly known. We coupled biotelemetry observations of black sea bass in the U.S. Mid-Atlantic Bight with numerical modelling of the coastal ocean to evaluate the influence of Hermine (3–8 September 2016) on cold pool thermal destratification and fish evacuation. Spring through fall, black sea bass is a sedentary species, with movements focused on structure where they support important commercial and recreational fisheries. During summer 2016, we characterized the movements of 45 acoustically tagged black sea bass at three sites deploying acoustic receivers moored in shelf waters 18–31 km east of Ocean City, Maryland, and at depths 20–32 m in the southern Mid-Atlantic Bight. On 3 September 2016, cyclonic winds of Hermine caused rapid destratification of the water column. At experimental sites, bottom temperatures rose from 13 to 23°C in 10 h. An oceanographic model and observing data showed that the effects of this destratification dominated large portions of the Mid-Atlantic Bight and had long term effects on seasonal evolution of the shelf temperature. Nearly half of remaining black sea bass on 3 September (40%) permanently evacuated the experimental sites. Those that remained showed long-term depressed activity levels. Although the cause of this incomplete evacuation is unknown, it exemplifies partial migration, which may buffer black sea bass to regional impacts of changed timing or increased incidence of tropical storms.

Keywords: cold pool, destratification, evacuation, hurricane, Mid-Atlantic Bight, migration, regional ocean model, telemetry.

Introduction

An important class of fish migration is evacuation: a sudden collective response to extreme changes in environmental conditions (Dolloff *et al.*, 1994; Secor, 2015). Evacuations can occur as an escape to catastrophic events such as volcanic eruptions and storms, and result in novel migration behaviours (DeVore *et al.*, 1999; Bailey and Secor, 2016). Evacuations can also occur in response to regularly recurring events. Wholesale advective evacuations from island streams to coastal waters occur every generation by fish larvae for a large group of small-bodied taxa classified as amphidromous; these fish then recolonize the same watersheds (McDowall, 2007). Winter seasonal emigration in temperate rivers and estuaries, stimulated by rapid drops in temperature, also resemble evacuation behaviours. Evacuations may thus represent

(i) extreme and novel behaviours driven by catastrophic events or (ii) seasonally or generationally recurring migrations influenced by rapid but periodic changes in the environment. Further, evacuations may be incomplete and represent a type of partial migration (Secor, 2015), whereby multiple behavioural modes can influence how populations respond to catastrophes and seasonal and generational changes to the environment.

Productive shelf ecosystems are regions of mixing and seasonal transition providing the greatest portion of the world's fishery yield, yet they are also prone to extreme environmental changes owing to estuarine discharges, weather events, and seasonal changes in circulation and warming (Gong *et al.*, 2010; Glenn *et al.*, 2016). The US Middle Atlantic Bight (MAB) is a large shelf region (~50–200 km wide) extending from the southern edge of

Georges Bank to Cape Hatteras. As a temperate region, it is influenced by sub-arctic and sub-tropical coastal currents with large seasonal oscillations ($\Delta 18^\circ\text{C}$) in sea surface temperature (He *et al.*, 2010; Richaud *et al.*, 2016). High rates of surface warming and reduced winds in spring produce a thermocline over most of the shelf, resulting in strong density stratification and entrapment of thick bottom layer of winter water bounded by mixed inner shelf water at depths $<10\text{--}20\text{ m}$ and the shelf break front that partitions saltier slope water (Houghton *et al.*, 1982; Sha *et al.*, 2015; Lentz, 2017). This mass of remnant winter water, known as the cold pool, persists throughout the summer, recharged by residual bottom currents from the Gulf of Maine and northward (Houghton *et al.*, 1982; Rasmussen *et al.*, 2005). The cold pool erodes in fall with cooling inshore and surface waters, increased winds, and thickening of the mixed layer depth, but can be accelerated by summer and fall storm events (Castelao *et al.*, 2010; Gong *et al.*, 2010; Lentz, 2017). Storms can cause rapid destratification in the MAB, resulting in extreme temperature change throughout the water column as summer surface water mixes with remnant sub-pycnocline winter water (Glenn *et al.*, 2016; Miles *et al.*, 2017; Seroka *et al.*, 2017).

Here we report on the evacuation behaviours by a common and exploited demersal species, black sea bass *Centropristis striata*, caused by a storm-driven destratification event in the southern portion of the MAB. Tropical cyclones, including hurricanes, can bring catastrophic changes to fish and fisheries, yet they recur with some degree of seasonal regularity. Indeed, the topical question on whether cyclone frequency has increased as a result of climate change has been difficult to resolve owing the historical regularity of cyclone incidence (Holland and Webster, 2007; Knutson *et al.*, 2010; Coumou and Rahmstorf, 2012). Thus, cyclone-driven evacuations may alternatively represent novel escape behaviours to extreme events or seasonal migrations driven by recurring changes, such as massive water column destratification, each fall.

As a temperate reef species, black sea bass are sedentary for most of the year in inner and mid-shelf regions of the MAB, undertaking winter migrations to outer shelf regions (Fabrizio *et al.*, 2013). During spring, summer, and fall, older juveniles,

and adults adopt home ranges between 0.3 and 2.0 km^2 (mean $\sim 1.0\text{ km}^2$) often focused on both natural and artificial bottom structure (Fabrizio *et al.*, 2014). Home ranges are likely related to their hermaphroditic protogynous mating system, where dominant large males establish territories to limit access to multiple females (Nelson *et al.*, 2003). Fisheries target hard bottom habitats and tend to selectively remove larger males (Provost, 2013), which may disrupt mating systems (Brooks *et al.*, 2008), although a sub-ordinate male ecomorph may partially offset fishing influences on reproductive success (Blaylock and Shepherd, 2016). The species ranges widely from the Gulf of Mexico to recent incursions into the Gulf of Maine, which may be related to regional warming (NEFSC, 2017). As such it tolerates a wide range of temperature conditions given sufficient acclimation (Musick and Mercer, 1977). Black sea bass in the northern MAB (north of Hudson Canyon) undertake southerly offshore winter migrations; those in the southern MAB are thought to seasonally migrate in an offshore direction only (Moser and Shepherd, 2009; Miller *et al.*, 2016).

We coupled biotelemetry observations of black sea bass and bottom temperatures with a Finite-Volume Community Ocean Model (FVCOM) of the MAB to evaluate the influence of Hermine (3–6 September 2016) on cold pool destratification and fish evacuation. The two approaches provided a means to remotely assess oceanographic forcing and fish behaviours during a period when sea state prohibited direct observations. Further, new developments in acoustic biotelemetry allow simultaneous logging of high frequency movements and bottom environmental conditions. The FVCOM permitted broader exploration of the influence of Hermine on ocean destratification and predictions of the spatial and temporal extent of the storm's influence on environmental and circulation features within the MAB.

Methods

Biotelemetry

Three biotelemetry sites were selected on one natural reef and two ship wrecks in shelf waters $18\text{--}31\text{ km}$ off the coast of Maryland (Figure 1a). These sites ranged $20\text{--}32\text{ m}$ in depth (Table 1) and were known by the contracted charter fisher to

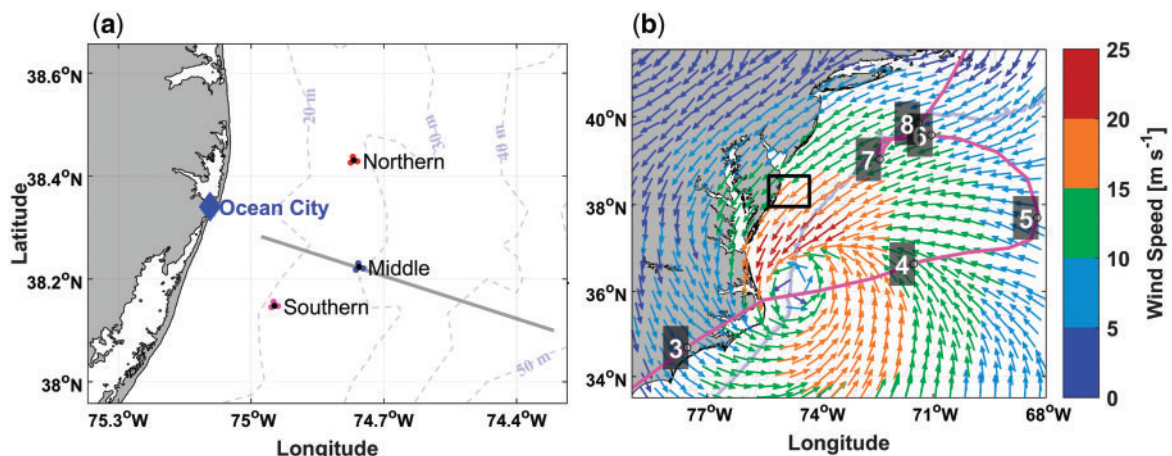


Figure 1. (a) Biotelemetry study sites and bathymetry in the southern Middle Atlantic Bight. Each study site is characterized by a release location (central black circle) and three surrounding acoustic receivers (surrounding circles). The cross-shelf section used for the modeling analysis is marked by the thick gray line. (b) A snapshot of Hermine's surface wind at 13:00 LST on 3 September. The empty box marks the location of the study sites. The track of Hermine is shown as the thick line where the time stamps of the storm center are marked by days (in LST) in September 2016.

Table 1. Acoustic receiver deployment depths and weights and total lengths of black sea bass (\pm SD) released at three biotelemetry sites ($n = 15$ at each site).

Site	Depths (m):		
	0°, 120°, 240°	Weight (g)	Total Length (mm)
Northern	26, 22, 26	201.3 \pm 92.0	259.6 \pm 24.9
Middle	26, 32, 22	266.7 \pm 106.3	271.3 \pm 30.6
Southern	20, 20, 20	263.3 \pm 81.2	267.8 \pm 24.3
All		245.1 \pm 95.9	265.6 \pm 26.3

harbour high densities of black sea bass. Each site was surrounded by relatively flat seabed dominated by sand and silt (>90%; Steimle and Zetlin, 2000; Guida *et al.*, 2015). Sites were originally selected to evaluate how black sea bass respond to noise emanating from construction of a meteorological tower, which was to assess wind fields in advance of offshore wind turbine installations. Construction of the tower was delayed, but the design provided three replicates to evaluate movement behaviours owing to oceanographic forcing.

Each of the three sites comprised a tag-and-release central location surrounded by three receivers, each 800 m from the release location at 0°, 120°, and 240° headings and thus providing a triangular acoustic corral about the reef and released fish. The 800 m distance was supported by acoustic tag detection distances (Fabrizio *et al.*, 2014) and resulted in 6.0 km² areal detection centered on each release location [3 receivers \times $\pi(0.8 \text{ km})^2$]. Fifteen fish were implanted with transmitters and released and three receivers were deployed at each site during 9–12 June 2016.

To avoid subsequent retention by fishers, fish were selected below the legal size limit (32 cm total length). Capture of equal or greater number of larger fish at these same sites indicated similar habitat selection between small and large adults. The minimum suitable size tagged (based on the relative size of the implanted tag) was 21 cm total length (Table 1). V9-2H (VEMCO, Ltd) transmitters were selected based on their small size (20 mm long and 9 mm diameter) and high power output, which permitted a greater detection range. Lengths and weights did not vary between sites (ANOVA: $p > 0.1$; Table 1). After capture by hook and line, fish were held in a pre-surgery tank prior to anesthetization and surgery. Fish were placed in a bath of 20 mg/l AQUIS 20E anesthetic (AQUIS New Zealand Ltd) for 2–20 min until respiration slowed and the fish lost equilibrium. Surgical procedures (20 mm incision, 1–2 single interrupted sutures) occurred while the fish was immersed and required 2–4 min (Table 1). Lengths, weights, and to the extent possible sex was identified by inspection through the incision. Fish were allowed to recover equilibrium in a separate tank and then released at 50% of the depth of capture by a special fishing rig (<http://seaqualizer.com/>) to promote recovery from barotrauma.

We used acoustic-release receivers (VEMCO, Ltd VR2AR) attached to a sacrificial weight (two 20.5 kg steel plates) and a 25-cm diameter hard trawl float. Receivers were 1-m above the seabed and logged temperature, ultrasonic noise (69 khz), and tilt angle every hour. Receivers were retrieved and redeployed on 3–4 August, 1–2 November 2016, and 3–4 May 2017.

Ocean model

A Finite Volume Coastal Ocean Model (FVCOM) was used to synoptically evaluate the influence of cyclone forcing on MAB

oceanography (Lee *et al.*, 2017; Zhang *et al.*, 2017). The hydrodynamic model comprises a series of 3-D equations for momentum, continuity, temperature, salinity, and density constrained by the Mellor-Yamada level 2.5 turbulent closure scheme (Chen *et al.*, 2003). FVCOM was initialized on 1 January 2016 with temperature, salinity, and sea level obtained from Experimental System for Predicting Shelf and Slope Optics (ESPreSSO, <http://www.myroms.org/espresso/>). Configured for the entire MAB shelf's bathymetry (Supplementary Figure S1) and with 5 km triangular grid elements, the model was forced by surface heat and momentum fluxes from the North American Mesoscale forecast system. The open boundary conditions were prescribed using the temperature, salinity, and subtidal sea level from Hybrid Coordinate Ocean Model and Navy Coupled Ocean Data Assimilation systems (HYCOM-NCODA, <http://hycom.org>), and five major tidal constituents from the Oregon State University TOPEX/Poseidon Global Inverse Solution TPXO 7.1 (Egbert *et al.*, 1994; Egbert and Erofeeva, 2002). A central location and bisecting transect within the study area were, respectively, chosen for time-series and cross-sectional depictions of coastal destratification (Figure 1a). Model skill in temperature and regional surface current predictions were evaluated, respectively, with receiver and satellite observed temperatures, and HF-Radar observed currents (see Supplementary Material).

Statistical analysis

Loss and movement rates were evaluated for the period 9 June to 31 December, the latter date representing a winter date when all fish were expected to have migrated offshore (Miller *et al.*, 2016). Evacuation was tested as an abrupt change in fish presence in contrast to background losses resulting from exploitation (fish growing into the fishery or landings of undersized fish), predation, or individual movements away from the site, which may be density-dependent. Loss rate was modelled by accumulating individuals over the duration of their occupancy (last detection date) and regressing this number of individuals versus date. Difference between sites in background loss rate was tested through analysis of covariance.

Evacuations in the daily time series of individual fish in each array were tested with intervention analysis using the *tsoutliers* package in R (López-de-Lacalle, 2017; R Core Team, 2017). This is a recursive modeling procedure that involves (i) time series fitting and (ii) adjustment of the fitted time series for identified outliers (“interventions”). Model-fitting iterations were ceased when no additional interventions were identified. Since each series exhibited inconsistent statistical properties through time and lacked stationarity (augmented Dickey-Fuller test: $p > 0.05$), time series were fitted using autoregressive integrated moving average (ARIMA) models as determined by Akaike Information Criterion. We tested interventions in the modelled time series as two classes of shifts: (i) a constant permanent shift, and (ii) a temporary shift, which reverts to the original time series state. To include only the largest interventions, outliers were identified as those points with a standardized t-statistic (Chen and Liu, 1993) > 5 . The permanent shift represented large loss events (evacuations), while the temporary shift represented either a short term displacement of fish or temporary reduction in acoustic receiver performance owing to ocean noise. High current and wind activity associated with storms resulted in increased ultrasonic noise (69 khz), which interfered with transmitter detections. Thus it

was important to evaluate time series separately for transient versus permanent changes in transmitter detections.

Activity levels were tested before and after Hermine using analysis of variance, blocking for site effects. Activity was estimated as the number of telemetry receivers that individual fish visited per hour. In analyzing activity levels, fish were classified as those that left prior to Hermine; those that remained until Hermine and evacuated; and those that remained after Hermine.

Results

Fish loss and activity rates

All tagged fish were subsequently detected except one released at the northern site, which was omitted in analysis on loss rates. Released fish were frequently detected within the acoustic corrals, with number of detections highest for the southern (324, 898) and northern (212, 560) sites and lowest for the middle site (111, 796). Analysis of covariance detected significant differences in loss rate between sites ($p < 0.001$). Loss rates were relatively constant throughout the study period (Figure 2) and were lowest at the southern site ($0.073 \text{ fish d}^{-1}$; $-0.5\% \text{ d}^{-1}$), intermediate at the northern site ($0.099 \text{ fish d}^{-1}$; $-0.7\% \text{ d}^{-1}$), and the highest at the middle site ($0.115 \text{ fish day}^{-1}$; $-0.8\% \text{ d}^{-1}$). Overall loss rate for all sites was 0.25 fish d^{-1} ($-0.6\% \text{ d}^{-1}$).

A large drop in number of detections and individuals present occurred on 3 September (Figures 2 and 3). Of those fish that remained until 3 September, 8 of 20 (40%) were subsequently not

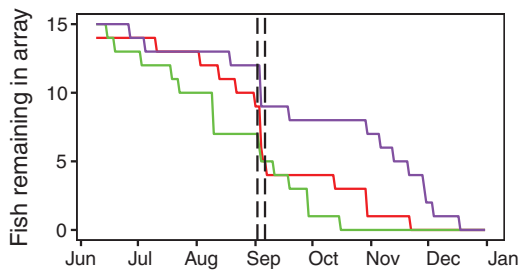


Figure 2. Loss in numbers of black sea bass across all sites and at each site for period 9 June to 31 December 2016. Following Hermine, lines representing sites are ordered from high (purple: southern), intermediate (red: northern), and low (green: middle) numbers of fish. For reference, dashed lines indicate 2–6 September.

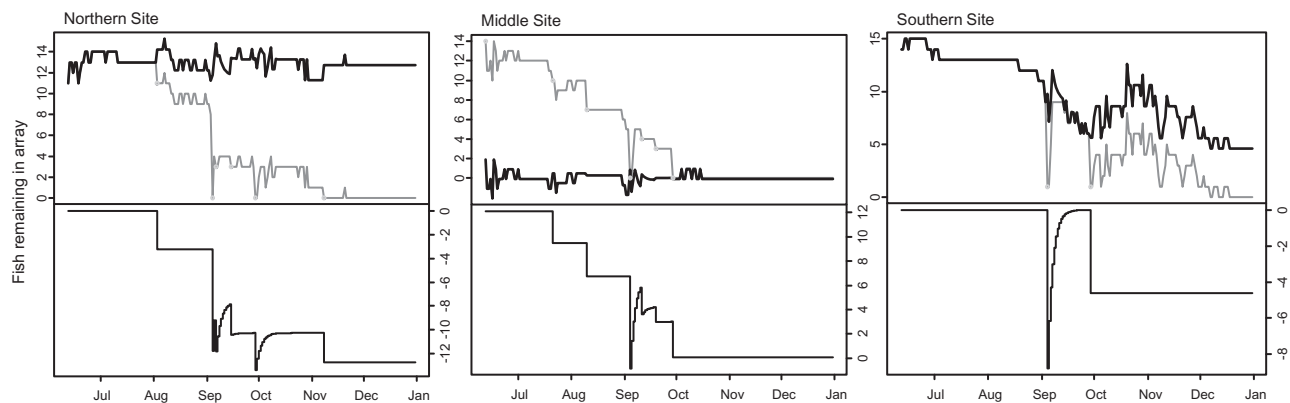


Figure 3. ARIMA intervention analysis of daily detections of individuals at each biotelemetry site. In the top panels, grey line indicates observed individual detections and the black solid line represents the ARIMA fitted time series. In the bottom panels, the black line indicates modelled temporary and permanent shifts in the time series, which are also shown as small circles in the observed time series.

detected. Evacuation numbers varied between sites with highest numbers at the northern and southern sites, and lower numbers at the middle site (Figures 2 and 3). Individuals that evacuated were not significantly different in length or weight as those that remained (ANOVA: $p > 0.05$ for both length and weight). ARIMA intervention analysis detected both temporary and permanent shifts in time series at all sites. The Northern and Middle sites were well fitted by ARIMA models, as shown by modelled stationarity (augmented Dickey-Fuller test: $p < 0.01$; black lines, Figure 3 and Table 2). The Southern site, by this diagnostic, was poorly fit and the modelled time series did not attain stationarity (augmented Dickey-Fuller test: $p > 0.05$). Although multiple shifts occurred in each time series (Table 2), large amplitude shifts were consistently associated with Hermine. On 3 September, large temporary shifts were detected at all sites, likely related to high ocean noise and reduced acoustic receiver performance. On this same date, a large spike in 69 kHz noise was recorded at all sites (see Figure 6). The temporary shift was followed by a permanent loss in detections, the timing of which varied between sites, occurring immediately following the temporary shift at the northern site, but lagging 7 and 25 d at the middle and southern sites (Table 2). Other shifts in the time series were inconsistent between sites, with the northern and middle sites showing early and late permanent shifts, and the southern site showing a more-variable rate of loss without evidence of large shifts outside that associated with Hermine.

Activity rates varied significantly before and after Hermine ($p = 0.002$), with post-event rates declining by 5-fold (Figure 4). Remarkably, post-event activity rates remained low until the end of the study period (30 December). Pre-event activity between those fish that evacuated after 3 September and those that remained after Hermine did not significantly vary ($p > 0.1$). Activity rates were unrelated to length or weight (regression: $p > 0.1$ for both length and weight).

Observed bottom temperature, noise, and tilt angle

Logged bottom temperature, ultrasonic noise, and tilt angle all showed evidence of Hermine on 3 September. Bottom temperatures remained low at all sites during July and August (Figure 5). Higher temperatures occurred at the shallower southern site (14.3 ± 1.3 (SD) °C) than those at either the middle (12.5 ± 1.0 °C) or northern site (12.1 ± 1.1 °C). Temperatures changed abruptly on 3 September,

Table 2. Results from the ARIMA intervention analysis on northern, middle, and southern site time series of black sea bass hourly detections.

Site	ARIMA model estimates (± 1 s.e.)	Date	Shift	Loss (± 1 s.e.)
Northern AR Model (2, 0, 0)	AR1 = 0.59 ± 0.074	2 Aug	Permanent	-3.24 ± 0.34
	AR2 = 0.09 ± 0.080	3 Sep	Temporary	-8.53 ± 0.58
	Intercept = 12.94 ± 0.26	5 Sep	Permanent	-4.38 ± 0.43
		14 Sep	Permanent	-2.64 ± 0.41
		28 Sep	Temporary	-3.10 ± 0.61
Middle AR Model (0, 0, 0)	None (white noise)	7 Nov	Permanent	-2.47 ± 0.31
		11 Jun	Permanent	12.01 ± 0.08
		20 Jul	Permanent	-2.60 ± 0.14
		9 Aug	Permanent	-2.78 ± 0.15
		3 Sep	Temporary	-7.55 ± 0.39
		10 Sep	Permanent	-2.48 ± 0.20
		18 Sep	Permanent	-1.23 ± 0.24
Southern AR Model (1, 1, 1)	AR1 = 0.42 ± 0.12	28 Sep	Permanent	-2.94 ± 0.17
	MA1 = -0.73 ± 0.082	3 Sep	Temporary	-8.78 ± 0.87
		28 Sep	Permanent	-4.61 ± 0.77

Model selection specifies inclusion of autoregressive (AR), differencing (D), and moving average terms (MA). AR = ARIMA model order; All ARIMA model and loss estimates significant at $p < 0.001$.

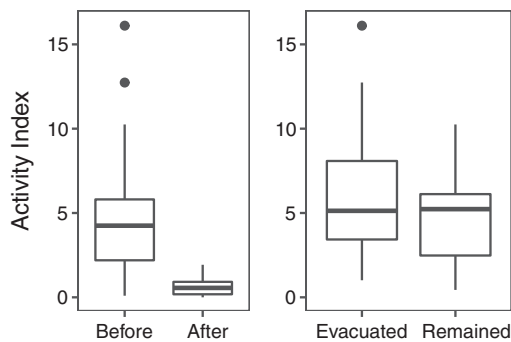


Figure 4. Box whisker plots of activity indices (receivers visited per hour) for combined sites. Left panel compares activity levels before and after 3 September (Hermine) across all sites. Right panel compares movements of individuals prior to 3 September that evacuated or remained at the site following 3 September.

increasing from 13 to 23°C in 10 h at the northern and middle sites (3 Sep, 16:00 to 4 Sep, 04:00) and from 14 to 23°C in 20 h at the southern site (3 Sep, 01:00 to 21:00) (Figures 5 and 6). Temperatures converged among sites and remained at high levels (20–23°C) until early October and thereafter steadily fell for the remainder of fall (Figure 5).

Logged ultrasonic frequencies recorded storm wind stress, which produces noise over a broad spectrum (Knudsen *et al.*, 1948; Hildebrand, 2009). Peaks in ultrasonic noise coincided with Hermine across all sites, ramping up during the second half of 3 September, and then maintaining strength until the second half of 6 September (Figure 6). Tilt angle, an index of bottom currents to which the moored receiver is exposed, showed increased angles during the same 3–6 September period (Figure 6).

FVCOM modelling of Hermine’s impact on the MAB

Hurricane Hermine formed as a tropical depression in the Straits of Florida on 28 August (NWS, 2017). A high pressure cell over continental US deflected the depression westward into the Gulf of Mexico where it strengthened into a Hurricane (wind speed 120–130 km h⁻¹) and made landfall 4 d later on Florida’s panhandle.

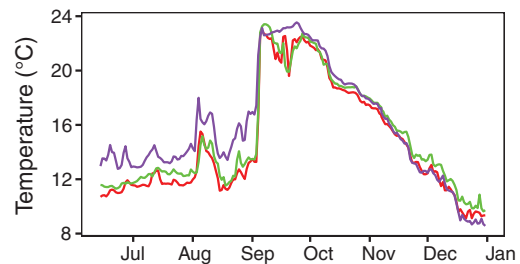


Figure 5. Logged daily bottom temperatures at each biotelemetry site. Sites are represented as purple (southern), green (middle), and red (northern) lines. Temperatures at each site represent the average of three acoustic receivers.

The cyclone traversed rapidly through continental SE US, diminished to a Tropical Storm, and first moved into the MAB on 13:00 LST 3 September just North of Cape Hatteras (Figure 1b). Hermine again strengthened and transited over the southern MAB shelf for 24 h (wind speed 111 km hr⁻¹), and then took an unusual path to the northwest during 4–5 September (wind speed 102–111 km h⁻¹), persisting in MAB shelf, slope, and offshore waters until 8 September (Figure 1b).

Prior to the arrival of Hermine, model results for a cross-shelf section through the middle telemetry site in the southern MAB clearly showed a thermocline delimiting surface warm (~20–25°C) waters over the cold pool (~8–12°C) bounded at 15–20 m depth (Figure 7). The water column quickly destratified in the inner to mid-shelf between 3 September and 4 September in concert with the strong southward longshore currents driven by northerly winds in the right quadrants of the storm (Figure 8). Near the end of the storm’s passage through the study area, temperature was vertically uniform across the inner and mid-shelf, extending from the coastline to 40 km offshore (Figure 7c–e), while strong southward currents occupied the entire water column (Figure 8c and d). The model-predicted time series at the middle telemetry site provided detailed depiction of the temporal evolution of temperature, salinity, and velocity field (Supplementary Figure S2). Both temperature and salinity became vertically homogeneous after 00:00 LST 4 September at the site. The temperature difference

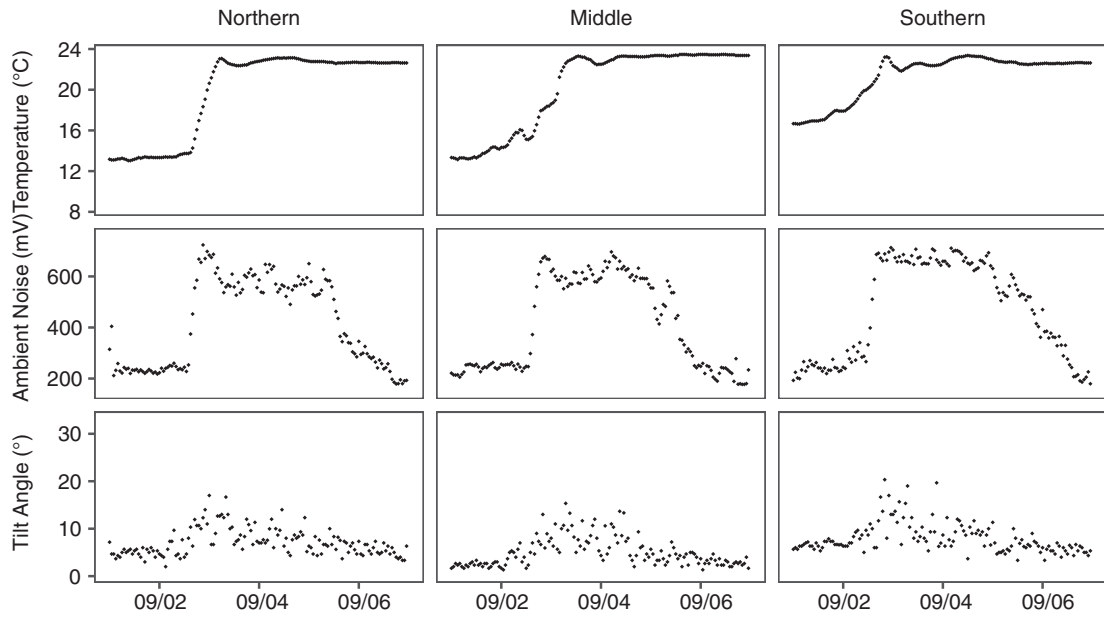


Figure 6. Hourly logged bottom temperature, 69 kHz noise, and tilt angle for the three biotelemetry sites during the passage of Hermine. Values for each site represent the average of three acoustic receivers.

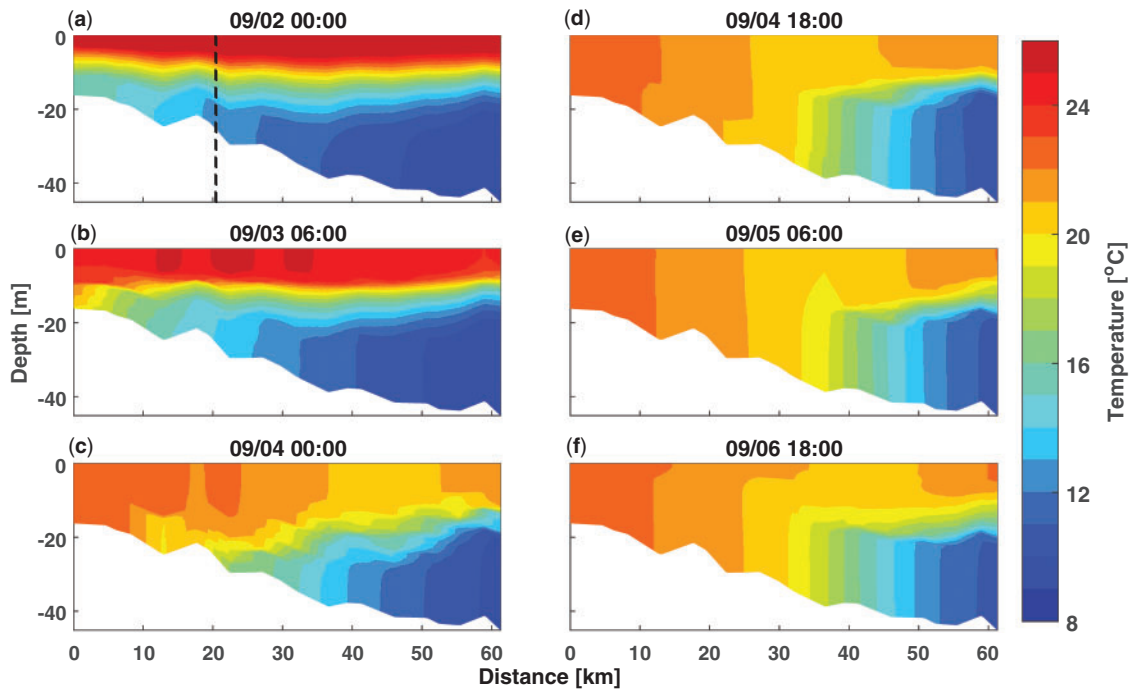


Figure 7. Model-predicted temperature distributions in a cross-shelf section through the middle telemetry site: (a) before the arrival of Hermine; (b–e) during the passage of Hermine; (f) after the storm. The dashed black line in the upper-left panel marks the position of the middle telemetry site shown in Figure 1.

between the surface and bottom waters at the reference site was 14°C before the arrival of Hermine but reduced to zero over a period of 10–12 h, indicating a rapid vertical-mixing process. Destratification resulted in erosion of the thermocline with complete homogenization of the water column by 12:00 LST on 4

September to an intermediate temperature of around 22°C at the middle telemetry site (Figure 9). The model-predicted temperature increased from 13.5 to 22°C over a time span of 24–30 h, in good agreement with the observed temperature increase in the bottom water (Figure 9, dashed line).

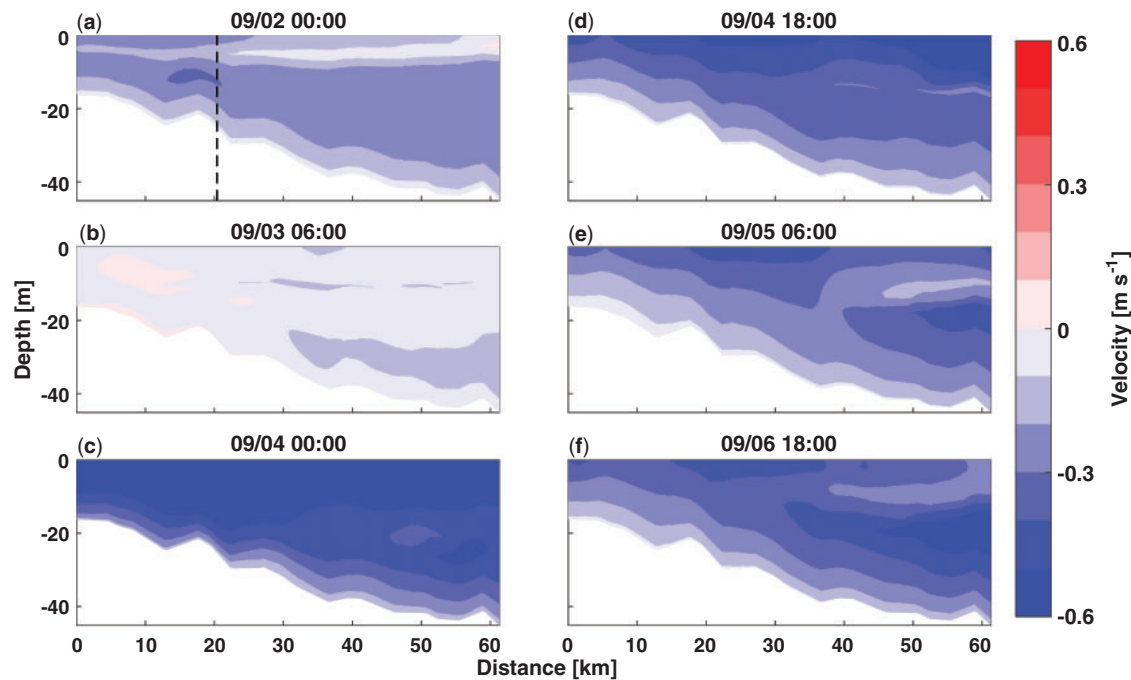


Figure 8. Model-predicted distributions of longshore currents in a cross-shelf section through the middle telemetry site: (a) before the arrival of Hermine; (b–e) during the passage of Hermine; (f) after the storm. Negative velocities indicate southern vector current.

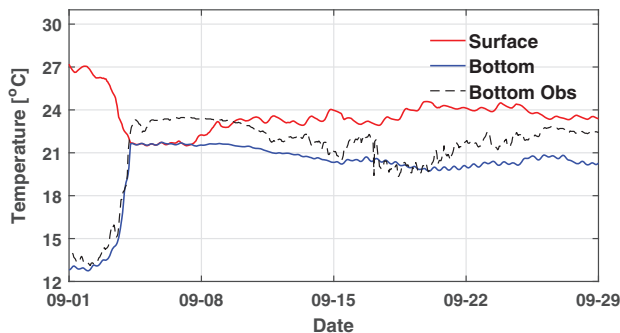


Figure 9. Model-predicted time series of surface (red; warmer series) and bottom (blue) temperature at the middle telemetry site during September 2016.

The strong northerly winds generated a two-layer downwelling circulation in the cross-shelf section, with onshore flows in the surface layer and offshore flows in the bottom layer, as shown in Figure 10. Since the bottom temperature was higher in the inner shelf than in the outer-shelf, the offshore currents advected warmer bottom water in the offshore direction and could have contributed to the bottom temperature increase at the telemetry sites. At the middle telemetry site, the average offshore current in the bottom water was 0.025 m/s and the cross-shelf temperature gradient was 0.5°C/km. Over a period of 24 h, this would cause a temperature increase of ~1°C. This is about one-tenth of the observed and predicted temperature increase (Figure 9). Therefore, at the shallow telemetry sites (20–25 m depth), vertical mixing rather than mass displacement appears to be the dominant mechanism causing the water column destratification and bottom temperature increase.

Although the three telemetry sites were located in a small area off the Ocean City, Maryland, the water-column destratification

and destruction of the cold pool occurred over a large area in the MAB impacted by Hermine (Figure 11). At 06:00 LST 3 September, when Hermine was located near the Outer Banks, North Carolina, the easterly winds in the front quadrants of the storm blew water against the Delmarva coastline and resulted in strong onshore flows. As Hermine made its way northward and offshore, the northerly winds in the right quadrants of the storm drove strong southward currents in the inner shelf. At this time, the strong southward current extended to the bottom. Figure 11 shows the distribution of top-to-bottom temperature difference ΔT during the passage of Hermine over the southern MAB. Initially $\Delta T \approx 0$ occurred only within 5 km from the coastline. However, the region with $\Delta T \approx 0$ expanded to over 60 km offshore and reached northward to the continental shelf off New Jersey. Similarly, the bottom water with warm temperature ($>20^\circ\text{C}$) greatly expanded in the southern MAB during the Hermine’s passage.

The model results indicated some recovery of the thermocline over the 2 weeks following Hermine (Figure 12), but the cold pool had dissipated. At the reference site, surface temperatures showed a threshold shift from 27 to 22°C, then increased slightly to 24°C, a level which persisted throughout September (Figure 9). The reestablished stratification was much weaker after the storm, with the top-to-bottom temperature difference recovering to 3°C, about 25% of the pre-storm value.

Discussion

Coupled telemetry and oceanography

In this linked analysis of telemetered black sea bass and modelled oceanographic forcing, we observed an evacuation behaviour caused by rapid increases in bottom temperature as the result of Hermine, water column destratification, and complete dissipation of the cold pool. Evacuation was supported by intervention

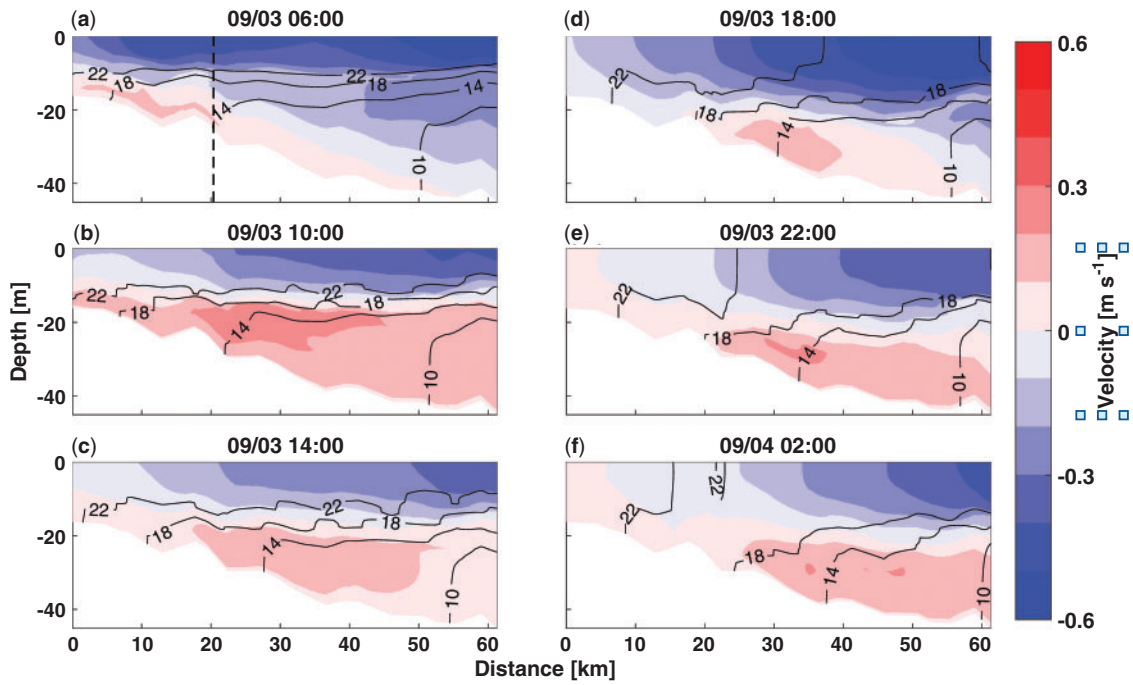


Figure 10. Model-predicted distributions of cross-shelf currents (positive for offshore velocity) and temperature (contours) in a cross-shelf section through the middle telemetry site: (a) before the arrival of Hermine; (b–e) during the passage of Hermine; (f) after the storm.

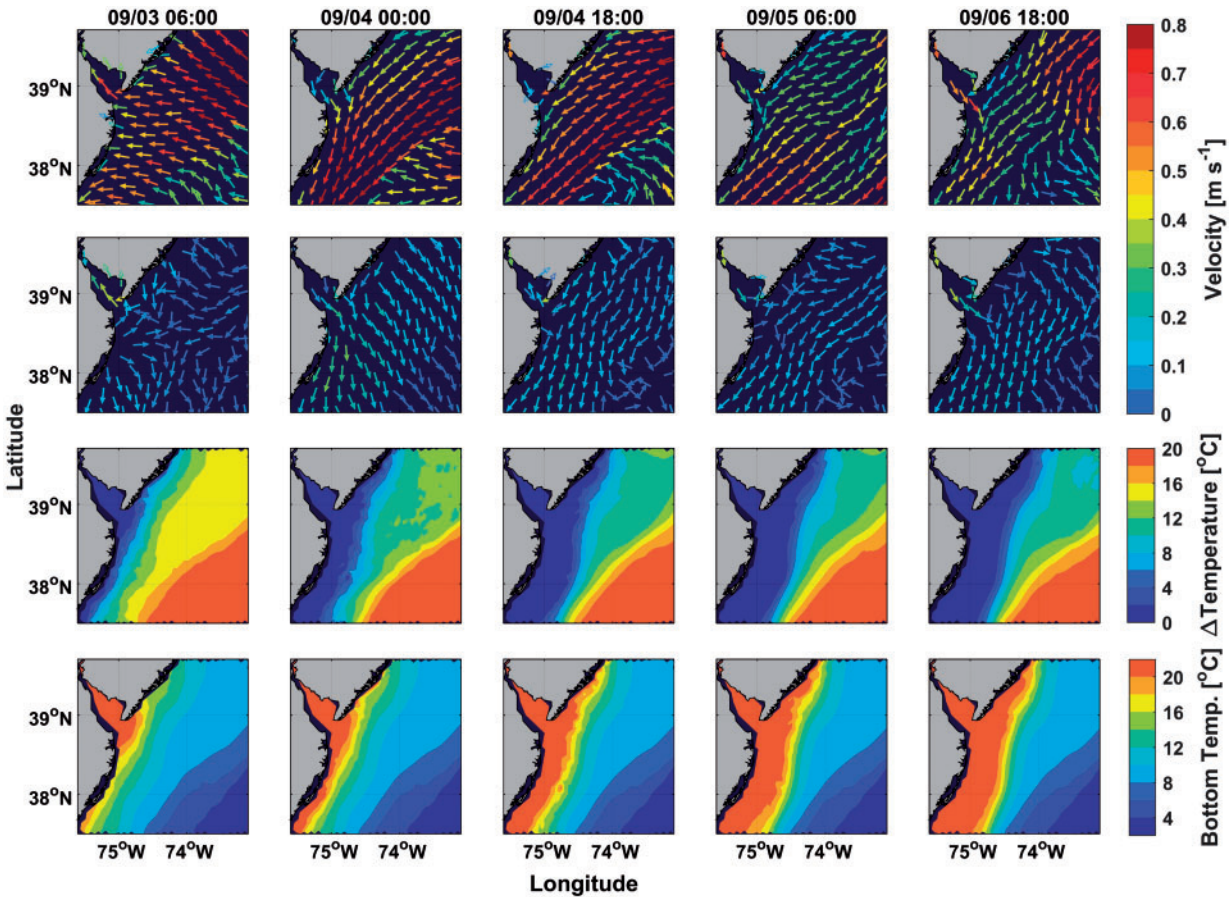


Figure 11. Model-predicted distributions of surface (top row), near-bottom (2 m above bottom; second row) currents, the differences between surface and bottom temperature (third row), and bottom temperature (bottom row) during the passage of Hermine.

analysis, which detected an abrupt level shift in the number of fish across all sites, albeit with differing levels of group movements. On the other hand, the majority of fish (60%) did not evacuate despite their exposure to changing bottom currents and temperatures that increased $>10^{\circ}\text{C}$ in a 10–20 h period. Those fish that persisted through Hermine and its aftermath exhibited greatly curtailed activity levels, possibly affecting their feeding and reproduction. The dual migratory and sedentary behaviours exhibited by black sea bass in response to a large episodic event represent a type of partial migration, whereby groups within populations express differing modes of migration behaviours. Such modalities may relate to size, sex, personality, or other latent propensities for certain spatial behaviours (Secor, 2015), although in this study we did not detect differences in evacuation behaviour related to fish size or movement activity levels prior to Hermine.

The FVCOM model results provided a unique means to evaluate the influence of Hermine and related wind stress on currents, temperature, and water column stratification. Further, the model allowed analysis of the spatial extent and duration of the storm's effect on ocean forcing and inferences related to the timing of destratification, longer term temperature changes, and the permanent dissipation of the cold pool. A further advantage of this and other regional ocean models is the ability to retrospectively compare the influence of tropical cyclones on MAB circulation patterns (Glenn *et al.*, 2016; Miles *et al.*, 2017; Seroka *et al.*, 2017). Hermine was not a particularly strong hurricane (NWS, 2017), but its track through the MAB was unusual. It would be valuable to use FVCOM realizations of other tropical storms through the MAB to evaluate whether predictions on destratification and cold pool dissipation can be made for classes of cyclones based on their seasonal timing, intensities, and storm tracks. Storm-induced mixing is thought to be a dominant mechanism for causing water-column destratification and bottom temperature increase on the continental shelf, but storm-driven downwelling circulation can advect warmer inner shelf bottom water in the offshore direction. Miles *et al.* (2017) showed that Hurricane Sandy advected the cold pool offshore by ~ 70 km. At the shallow telemetry sites in our study, however, our analysis suggests that the cross-channel advection only accounts for about 10% of the observed increase in the bottom temperature.

Bottom temperature, noise, and tilt angle data logged on the telemetry receivers were particularly valuable in providing highly resolved observed time series with which to compare FVCOM results (Supplementary Figure S3) and confirm inferences related to destratification. Observed bottom temperatures showed greater variation than the more modulated predicted thermal conditions but overall amplitudes of temperatures were quite similar (Figures 6 and 9 and Supplementary Figure S3). Environmental noise recorded at ultrasonic frequency corresponded to storm intensity (wind stress and sea state). These same periods of intense noise also interfered with transmitter signals, resulting in transitory changes in fish detection probabilities, which became apparent in our intervention analysis of fish numbers at each site (Figures 3 and 6). Tilt angles in excess of 10° occurred during this same period and corresponded to peaks in predicted bottom current velocities (Figure 6, Supplementary Figure S2). The environmental logging capabilities of the recent generation of telemetry receivers allowed important insights on ocean forcing that was unanticipated at the outset of the study. Remote observation data from HF-radar and an oceanographic buoy further supported FVCOM model realizations of changes in surface temperatures,

current fields, and water column destratification (Supplementary Figure S4).

Evacuation behaviours

A large sudden loss in black sea bass numbers occurred across the biotelemetry sites on 3 September, coincident with the passage of Hermine. This is most apparent in the cumulative loss for combined sites (Figure 2), which indicates the permanent loss of individuals from those sites. Intervention analysis gave more nuanced results owing to the storm's interference with transmitter signals. Temporary shifts (e.g. decreases in transmission detection rate) coincided with increased noise on 3 September. Detections showed permanent shifts following 3 September but varied in their lag from 2 d (northern site) to 25 d (southern site). We attribute some of this lag to model fitting, particularly for the southern site, for which the ARIMA model failed to stabilize the time series due to non-stationary increase and subsequent decrease in fish through October that could not be modelled as a point event (intervention). The presence of permanent shifts is supported by the analysis of cumulative fish loss, which showed a stepped decline on 3 September at all sites (Figure 2). Sites varied in loss patterns with the northern site showing the largest number of storm departures (-6) and the middle site showing the least (-2). Sites varied in bottom temperatures, which were 4°C warmer at the shallower southern site in comparison to the middle and northern sites. The larger change in temperature at the northern site may have caused increased evacuation with the passage of Hermine. Other changes in loss rate patterns between sites may relate to differences in fishing mortality as sites are likely to attract varying levels of exploitation. Fishing and other losses may also relate to local densities but were not monitored in this study so inferences on the fates of fish lost to the biotelemetry sites are limited. We were able to recover two fish the following spring (2017) recorded at the middle and outer sites, indicating site fidelity across years occurs for some fraction of the surviving fish.

Loss rate during summer by MAB black sea bass was similarly evaluated in a 2003 biotelemetry study on 122 black sea bass in 17–34 m depth water off the New Jersey coast (Fabrizio *et al.*, 2013, 2014). Low rates of loss occurred during summer months, followed by higher rates from September through December. Interesting, accelerated loss rates coincided with a sudden rise in bottom temperature (from c. 11 – 19°C) during mid-September, coincident to Hurricane Isabel, whose path passed the southern bordered of the MAB. Although the authors noted that no abrupt pulse of departures was associated with this temperature excursion, a notable change in loss rates was illustrated (Fabrizio *et al.*, 2013: Figure 4). No information could be found related to possible cold pool destratification during this period, so the potential impact of Hurricane Isabel, which made landfall in the southern MAB (North Carolina and Virginia), is speculative. Still, Hurricane Isabel strongly forced turnover within the Chesapeake Bay (Li *et al.*, 2007), and could have had similar impacts on portions of the MAB. Similar to our results, inter-annual site fidelity was observed for two of their study fish.

Diminished activity levels during and after the passage of Hermine showed that the thermal destratification resulted in very large behavioural changes (Figure 4). Remarkably, activity levels remained at very low levels for the next 2–3 months despite some return of bottom waters to cooler temperatures and expectations for continued reef-associated movements associated with feeding

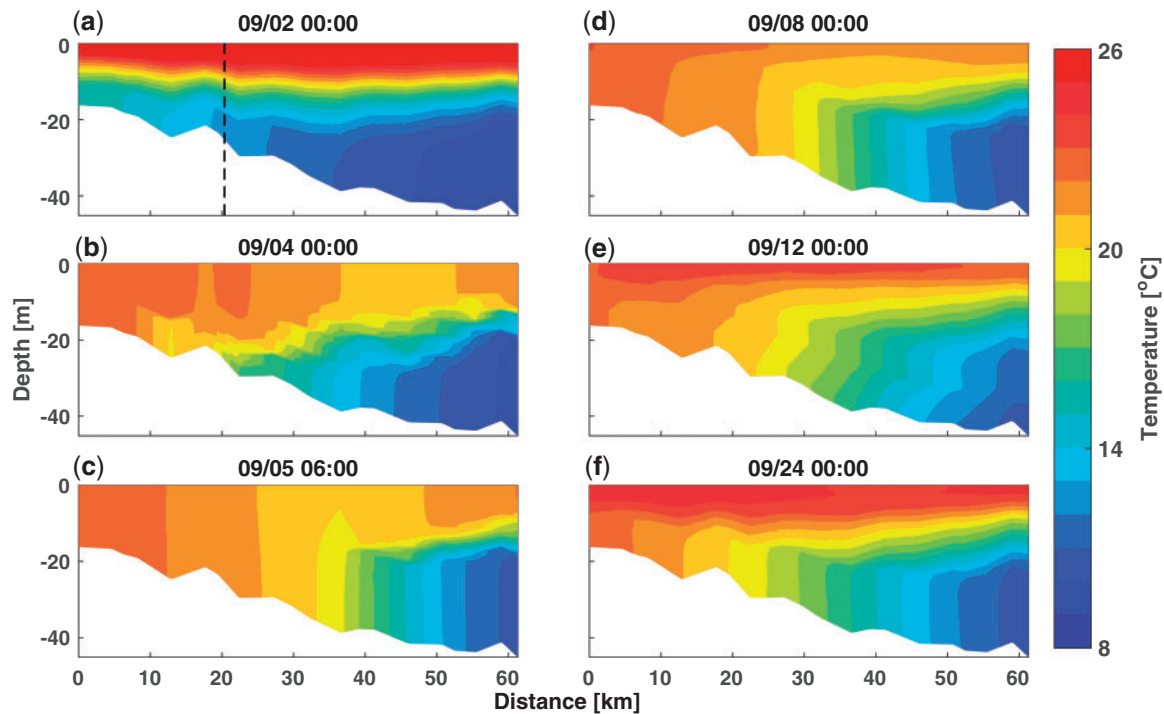


Figure 12. Long-term evolution of temperature distribution in a cross-shelf section through the middle telemetry site following the passage of Hurricane Hermine: (a) before Hermine's arrival; (b, c) during the passage of Hermine; (d–f) after Hermine's departure.

and reproduction. Activity levels, measured as the number of adjacent receivers visited per hour, followed an index developed by Fabrizio *et al.* (2014) in their black sea bass telemetry study. Interestingly, activity levels in that study showed a marked c. 3-fold decline (Fabrizio *et al.*, 2014; their Figure 7) in mid-September corresponding with the period of increased bottom temperatures. Correlates to activity level reported by Fabrizio *et al.* included interactions between sex, time of tagging and release, and bottom temperature. We did not detect changes in activity with fish size or propensity to evacuate. Still, our sample size was modest and we had only limited observations of sex, which was not included as a factor in our analysis.

Evacuation by black sea bass occurred during Hermine, simultaneous to large increases in temperature, noise and bottom currents. Temperature changes, c. 10°C in particular, would be expected to dramatically increase respiration and associated metabolic rates, likely reducing the scope for activity (Neill *et al.*, 1994; Niklitschek and Secor, 2009). Bottom reef structure may have alleviated the influence of flow, which otherwise would have required 1–2 body length s^{-1} swimming speeds (bottom currents measured 0.25–0.5 $m s^{-1}$; Figure 8) for fish to maintain position during the storm. Because cold pool destratification was extensive (Figure 11), evacuees would have had to swim large distances to encounter cooler waters in middle portions of the MAB (e.g. north of Delaware Bay) or towards the shelf break. Because black sea bass are eurythermal and occur over a wide latitudinal range, the physiology of those that remained likely acclimated, although their activity levels were permanently altered.

Storm-associated movements by coastal fishes have been rarely reported in the literature, and have been attributed to escape responses during and before storms cued by rapidly changing environmental conditions and physical displacement. Bailey and Secor

(2015) observed incomplete evacuations by Hudson River striped bass in response to two successive 2011 tropical storms (Irene and Lee), which caused rapid changes in temperature, salinity, and dissolved oxygen throughout the Hudson River estuary. A complete evacuation by telemetered juvenile blacktip sharks in advance of a Florida tropical storm was reported by Heupel *et al.* (2003), but departures were temporary with all individuals returning within 2 weeks to their nursery habitat. The authors suggested that evacuation was cued by a rapid drop in barometric pressure just prior to the storm. For tagged red snapper exposed to two large Gulf of Mexico hurricanes, net movements were two-fold higher than for fish that were not exposed to hurricanes (Patterson *et al.*, 2001). Displacements from tagging sites varied widely from nil to 352 km, but the large majority of storm-associated displacements occurred in a similar eastward trajectory.

The incomplete evacuation we observed due to Hermine may represent a type of partial migration, whereby individuals vary in their propensity to stay or leave. Evacuation by Hudson River striped bass varied by latent migration behaviours (i.e. contingent behaviours; Secor, 2015); individuals that were resident to the upper Hudson River estuary departed rapidly during storm events to coastal waters, whereas those resident to the lower estuary (NY Harbor) did not. Our study design (similar sized small adults, limited observations on sex, limited ability to evaluate the fate of evacuees) precluded inferences on demographic factors that led to the propensity to evacuate. We hypothesized that fish that showed higher levels of activity prior to Hermine would be prone to evacuate, but found no evidence for this (Figure 4). Fabrizio *et al.* (2014) detected no overall influences of sex and size on black sea bass activity levels in their study, but did observe seasonal changes in activity, which they attributed to increased activity levels by early arriving males, which ranged over larger home ranges than later arrivals.

Role of storms in destratification and fish migrations

Tropical storms and hurricanes are one of several factors contributing to permanent dissipation of the two-layered thermal structure of the MAB during late summer and fall months each year. Local thunderstorms can also temporarily dissipate stratification, as observed in early August, which was associated with an intense thunderstorm occurring on 1 August (Weather Underground, 2016). In contrast, tropical cyclones by themselves can induce very rapid changes in thermal structure over the large portions of the MAB and in some instances accelerate fall turnover. Their influence will depend on their path, timing, strength, and preconditioning factors such as previous climatology and storm incidence. Comparative studies provide important perspective on the influence of seasonal timing on storm impacts. Irene, an early September tropical storm (2011), caused large deepening (destratification) of the surface layer resulting in surface cooling. This in turn, diminished the strength of the storm prior to making landfall (Glenn *et al.*, 2016; Seroka *et al.*, 2017). As a late fall storm (October 2012) Hurricane Sandy succeeded seasonal cooling of the surface layer and maintained its strength as it made landfall, probably related to offshore advection of the cold pool by downwelling circulation (Miles *et al.*, 2017). Hurricane Arthur (July 2014) rapidly moved through the entire MAB region in <24 h; it had demonstrable but small effects on surface layer deepening (Glenn *et al.*, 2016). Hermine was an unusual storm in its path and long duration over the MAB region. Further, it occurred at the end of a particularly warm summer in the MAB, which contributed to a larger thermal gradient between surface and bottom layers. Large-scale and fairly long-term (2–3 d) winds and currents associated with Hermine destratified much of the MAB, permanently dissipating the cold pool. It would be interesting to model classes of tropical cyclones based on historical observations to evaluate the likely role of storm timing, strength, and paths on accelerating fall turnover.

Whether storm-induced destratification of the MAB during summer-fall is temporary or permanent will have important implications for MAB coastal fish assemblages. Temporary cold pool disruptions may result in short-term departures and transitory changes in fish behaviours, whereas permanent seasonal changes, such as those observed in this study where thermal conditions are not seasonally recovered, could result in sudden long-term shifts in movements, feeding and reproductive behaviours, and food webs. Sullivan *et al.* (2005), for instance, attributed recruitment failure (poor juvenile survival) by yellowtail flounder in the MAB to cold pool turnover caused by two successive hurricanes during early September (Hurricanes Edouard and Hortense in 1996). Should storm-induced cold pool turnover increase with climate change owing to increased storm intensity or frequency, the timing of migration for black sea bass and other MAB species could be altered. Black sea bass and other species in the MAB are shifting their distributions poleward with warming temperatures (Nye *et al.*, 2009; Pinsky *et al.*, 2013; Walsh *et al.*, 2015; Miller *et al.*, 2016). Such shifts could be accelerated by tropical storms, which may bias movements into northern or outer shelf regions.

Incomplete evacuation behaviours, related to propensities of different groups of fish to respond to environmental stresses, can result in ecological inertia to catastrophic (rapid destratification and bottom warming) or longer term (changed timing of cold pool turnover) changes. Evaluating these more-nuanced responses is important in understanding resilience by black sea bass and other MAB species to changed timing and possible increased incidence and

intensity of tropical storms. Telemetry approaches are now feasible in large and representative regions within the MAB on economically important species such as black sea bass. Coupled with oceanographic numerical models, detailed information on individual movement and collective migration behaviours can permit improved predictions on changed phenology and distributions associated with climate change and other anthropogenic stressors.

Acknowledgements

This study was supported by a grant by Maryland Department of Natural Resources and Maryland Energy Administration (14-16-2151 MEA) to DHS and grants from NOAA (NA13OAR4830233) and Maryland Sea Grant (NA14OAR4170090) to M.L. FZ was supported by a Maryland Sea Grant Fellowship. Captain D. Stauffer (FV Fin Chaser), A. Horne, R. Brodnick, and C. Lozano assisted with field work.

Supplementary data

Supplementary material is available at the ICESJMS online version of the manuscript.

References

- Bailey, H., and Secor, D. H. 2016. Coastal evacuations by fish during extreme weather events. *Scientific Reports*, 6: 30280.
- Blaylock, J., and Shepherd, G. R. 2016. Evaluating the vulnerability of an atypical protogynous hermaphrodite to fishery exploitation: results from a population model for black sea bass (*Centropristis striata*). *Fishery Bulletin*, 114: 476–489.
- Brooks, E. N., Shertzer, K. W., Gedamke, T., and Vaughan, D. S. 2008. Stock assessment of protogynous fish: evaluating measures of spawning biomass used to estimate biological reference points. *Fishery Bulletin*, 106: 12–23.
- Castelao, R., Glenn, S., and Schofield, O. 2010. Temperature, salinity, and density variability in the central Middle Atlantic Bight. *Journal of Geophysical Research-Oceans*, 115.
- Chen, C., and Liu, L. 1993. Joint estimation of model parameters and outlier effects in time series. *Journal of the American Statistical Association*, 88: 284–297.
- Chen, C., Liu, H., and Beardsley, R. C. 2003. An unstructured grid, finite-volume, three-dimensional, primitive equations ocean model: application to coastal ocean and estuaries. *Journal of Atmospheric and Oceanic Technology*, 20: 159–186.
- Coumou, D., and Rahmstorf, S. 2012. A decade of weather extremes. *Nature Climate Change*, 2: 491–496.
- DeVore, J. D., James, B. and Beamesderfer, R., 1999. Lower Columbia River white sturgeon: current stock status and management implications. Washington Department of Fish and Wildlife. Report No. SS 99–08.
- Dolloff, C. A., Flebbe, P. A., and Thorpe, J. E. 1994. Salmonid flexibility: responses to environmental extremes. *Transactions of the American Fisheries Society*, 123: 606–612.
- Egbert, G. D., Bennett, A. F., and Foreman, M. G. 1994. TOPEX/POSEIDON tides estimated using a global inverse model. *Journal of Geophysical Research: Oceans*, 99: 24821–24852.
- Egbert, G. D., and Erofeeva, S. Y. 2002. Efficient inverse modeling of barotropic ocean tides. *Journal of Atmospheric and Oceanic Technology*, 19: 183–204.
- Fabrizio, M. C., Manderson, J. P., and Pessutti, J. P. 2013. Habitat associations and dispersal of black sea bass from a mid-Atlantic Bight reef. *Marine Ecology Progress Series*, 482: 241–253.
- Fabrizio, M. C., Manderson, J. P., and Pessutti, J. P. 2014. Home range and seasonal movements of Black Sea Bass (*Centropristis striata*) during their inshore residency at a reef in the mid-Atlantic Bight. *Fishery Bulletin*, 112: 82–97.

- Glenn, S. M., Miles, T. N., Seroka, G. N., Xu, Y., Forney, R. K., Yu, F., Roarty, H., Schofield, O., and Kohut, J. 2016. Stratified coastal ocean interactions with tropical cyclones. *Nature Communications*, 7: 1–10.
- Gong, D., Kohut, J. T., and Glenn, S. M. 2010. Seasonal climatology of wind-driven circulation on the New Jersey Shelf. *Journal of Geophysical Research-Oceans*, 115.
- Guida, V., Drohan, A., Johnson, D., Pessutti, J., Fromm, S. and McHenry, J., 2015. Report on Benthic Habitats in the Maryland Wind Energy Area. NOAA/NEFSC/MD Interim Report to BOEM.
- He, R. Y., Chen, K., Moore, T., and Li, M. K. 2010. Mesoscale variations of sea surface temperature and ocean color patterns at the Mid-Atlantic Bight shelfbreak. *Geophysical Research Letters*, 37.
- Heupel, M. R., Simpfendorfer, C. A., and Hueter, R. E. 2003. Running before the storm: blacktip sharks respond to falling barometric pressure associated with Tropical Storm Gabrielle. *Journal of Fish Biology*, 63: 1357–1363.
- Hildebrand, J. A. 2009. Anthropogenic and natural sources of ambient noise in the ocean. *Marine Ecology Progress Series*, 395: 5–20.
- Holland, G. J., and Webster, P. J. 2007. Heightened tropical cyclone activity in the North Atlantic: natural variability or climate trend?. *Philosophical Transactions of the Royal Society a-Mathematical Physical and Engineering Sciences*, 365: 2695–2716.
- Houghton, R. W., Schlitz, R., Beardsley, R. C., Butman, B., and Chamberlin, J. L. 1982. The Middle Atlantic Bight cold pool: evolution of the temperature structure during summer 1979. *Journal of Physical Oceanography*, 12: 1019–1029.
- Knudsen, V. O., Alford, R. S., and Emling, J. W. 1948. Underwater ambient noise. *Journal of Marine Research*, 7: 410–429.
- Knutson, T. R., McBride, J. L., Chan, J., Emanuel, K., Holland, G., Landsea, C., Held, I., et al. 2010. Tropical cyclones and climate change. *Nature Geoscience*, 3: 157–163.
- Lentz, S. J. 2017. Seasonal warming of the Middle Atlantic Bight Cold Pool. *Journal of Geophysical Research-Oceans*, 122: 941–954.
- Lee, S. N., Li, M., and Zhang, F. 2017. Impact of sea-level rise on tidal ranges in Chesapeake and Delaware Bays. *Journal of Geophysical Research*, 122: 3917.
- Li, M., Zhong, L. J., Boicourt, W. C., Zhang, S. L., and Zhang, D. L. 2007. Hurricane-induced destratification and restratification in a partially-mixed estuary. *Journal of Marine Research*, 65: 169–192.
- López-de-Lacalle, J. 2017. *tsoutliers: Detection of Outliers in TimeSeries*. R package version 0.6-6. <https://CRAN.R-project.org/package=tsoutliers>.
- McDowall, R. M. 2007. On amphidromy, a distinct form of diadromy in aquatic organisms. *Fish and Fisheries*, 8: 1–13.
- Miles, T., Seroka, G., and Glenn, S. 2017. Coastal ocean circulation during Hurricane Sandy. *Journal of Geophysics Research Oceans*, 122: 7095–7114.
- Miller, A. S., Shepherd, G. R., Fratantoni, P. S., and Patterson, H. M. 2016. Offshore habitat preference of overwintering juvenile and adult black sea Bass, *Centropristis striata*, and the relationship to year-class success (vol 11, e0147627, 2016). *PLoS One*, 11: e0147627.
- Moser, J., and Shepherd, G. R. 2009. Seasonal distribution and movement of black sea bass (*Centropristis striata*) in the Northwest Atlantic as determined from a mark-recapture experiment. *Journal of Northwest Atlantic Fisheries Science*, 139: 241–256.
- Musick, J. A., and Mercer, L. P. 1977. Seasonal distribution of black sea bass, *Centropristis striata*, in Mid-Atlantic Bight with comments on ecology and fisheries of species. *Transactions of the American Fisheries Society*, 106: 12–25.
- National Weather Service. 2016. Hurricane Hermine. Report AL092016.
- Neill, W. H., Miller, J. M., van Der Veer, H. W., and Winemiller, K. O. 1994. Ecophysiology of marine fish recruitment: a conceptual framework for understanding interannual variability. *Netherlands Journal of Sea Research*, 32: 135–152.
- Nelson, D. A., Perry, D., and Baker, E. 2003. Natural spawning of black sea bass, *Centropristis striata*, at the NMFS Milford Laboratory and the UMASS Dartmouth laboratory with observations on spawning behavior. *Journal of Shellfish Research*, 22: 297–298.
- Niklitschek, E. S., and Secor, D. H. 2009. Dissolved oxygen, temperature and salinity effects on the ecophysiology and survival of juvenile Atlantic sturgeon in estuarine waters: II. Model development and testing. *The Journal of Experimental Marine Biology and Ecology*, 381: 161–172.
- Northeast Fisheries Science Center, National Marine Fisheries Service. 2017. 62nd Northeast Regional Stock Assessment Workshop. Assessment Report. Reference Document 17-03.
- Nye, J. A., Link, J. S., Hare, J. A., and Overholtz, W. J. 2009. Changing spatial distribution of fish stocks in relation to climate and population size on the Northeast United States continental shelf. *Marine Ecology Progress Series*, 393: 111–129.
- Patterson, W. F., Watterson, J. C., Shipp, R. L., and Cowan, J. H. 2001. Movement of tagged red snapper in the northern Gulf of Mexico. *Transactions of the American Fisheries Society*, 130: 533–545.
- Pinsky, M. L., Worm, B., Fogarty, M. J., Sarmiento, J. L., and Levin, S. A. 2013. Marine taxa track local climate velocities. *Science*, 341: 1239–1242.
- Provost, M. M. 2013. Understanding sex change in exploited fish populations: A review of east coast fish stocks and assessment of selectivity and sex change in black sea bass (*Centropristis striata*) in New Jersey. MS thesis. Rutgers University, New Jersey.
- R Core Team 2017. R: A language and environment for statistical computing. R Foundation for Statistical Computing, Vienna, Austria. <https://www.R-project.org/>.
- Rasmussen, L. L., Gawarkiewicz, G., Owens, W. B., and Lozier, M. S. 2005. Slope water, Gulf Stream, and seasonal influences on southern Mid-Atlantic Bight circulation during the fall-winter transition. *Journal of Geophysical Research-Oceans*, 110.
- Richaud, B., Kwon, Y. O., Joyce, T. M., Fratantoni, P. S., and Lentz, S. J. 2016. Surface and bottom temperature and salinity climatology along the continental shelf off the Canadian and US East Coasts. *Continental Shelf Research*, 124: 165–181.
- Secor, D. H. 2015. *Migration Ecology of Marine Fishes*. Johns Hopkins University Press, Baltimore. 304 p.
- Seroka, G., Miles, T., Xu, Y., Kohut, J., Schofield, O., and Glenn, S. 2017. Rapid shelf-wide cooling response of a stratified coastal ocean to hurricanes. *Journal of Geophysics Research Oceans*, 122: 4845–4867.
- Sha, J., Jo, Y. H., Yan, X. H., and Liu, W. T. 2015. The modulation of the seasonal cross-shelf sea level variation by the cold pool in the Middle Atlantic Bight. *Journal of Geophysical Research-Oceans*, 120: 7182–7194.
- Steimle, F. W., and Zetlin, C. 2000. Reef habitats in the Middle Atlantic Bight: abundance, distribution, associated biological communities, and fishery resource use. *Marine Fisheries Review*, 62: 24–42.
- Sullivan, M. C., Cowen, R. K., and Steves, B. P. 2005. Evidence for atmosphere-ocean forcing of yellowtail flounder (*Limanda ferruginea*) recruitment in the Middle Atlantic Bight. *Fisheries Oceanography*, 14: 386–399.
- Walsh, H. J., Richardson, D. E., Marancik, K. E., Hare, J. A., and Patterson, H. M. 2015. Long-term changes in the distributions of larval and adult fish in the northeast US shelf ecosystem. *PLoS One*, 10: e0137382.
- Weather Underground 2016. Ocean City, Maryland (KOXB). <https://www.wunderground.com/history/>.
- Zhang, F., Li, M., Ross, A. C., Lee, S. B. and Zhang, D.-L., 2017. Sensitivity analysis of Hurricane Arthur (2014) storm surge forecasts to WRF physical parameterizations and model configurations. *Weather Forecasting*, 32: 1745–1764.